Polymer Chemistry

ROYAL SOCIETY OF CHEMISTRY

PAPER

View Article Online
View Journal | View Issue

Check for updates

Cite this: *Polym. Chem.*, 2025, **16**, 2552

Sustainable one-pot synthesis of imide-containing polyesters with programmable structures and tunable performance†

Tianhua Ren, *[a,b,c] Feng Yu,[b,c] Jialong Li,[a,b,c] Jinlin Li[a,b,c] and Kechun Zhang*[b,c]

Received 25th February 2025,
Accepted 18th April 2025

DOI: 10.1039/d5py00190k

rsc.li/polymers

Sustainably producing thermoplastics with well-defined structures across various material chemistries remains challenging. Herein, we report a new synthetic methodology for thermoplastic polyesters with side-chain imide groups *via* one-pot melt polycondensation enabled by thermodynamic imide ring and ester formation, using either a two-component system of amino diol/dicarboxylic acid or a three-component system of amino diol/diol/dicarboxylic acid. Unlike traditional trifunctional systems, the amino groups of amino diols are fully converted into imide without cross-linking. This methodology was inspired by the model reaction of amino alcohol and dicarboxylic acid to form di(ester imide) *via* melt condensation, where the esterification, imidization and molecular chain propagation mechanisms can be extended to polymerization. The resulting series of imide-containing polyesters exhibited controllable weight-average molecular weights up to 110.8 kDa, a wide range of glass transition temperatures (–24.6 to 115.4 °C), and tunable mechanical properties with ultimate tensile strengths ranging from 8.0 to 34.5 MPa and elongations at break up to 472%. The programmable one-pot synthesis technology has extensive potential for sustainable and functional materials.

1. Introduction

Developing copolymerization technology that enables the one-pot conversion of a mixture of monomers into desirable and practically viable polymers has garnered considerable interest in commercial applications, as it combines the unique performance properties of each segment.[1–4] Copolymers are extensively utilized in various applications, including thermoplastic elastomers,[5–7] drug delivery systems,[8–10] hydrogels,[11,12] membranes,[13–15] and advanced plastics,[16–18] owing to the extraordinary controllability of their composition, molecular weight, molecular weight distribution, and structural configurations. Theoretically, it is feasible to synthesize polymers with any molecular architecture and combination, driven by potentially compelling structures and properties.[2] The one-pot synthesis of well-defined polymers by integrating multiple chemically distinct blocks and block types is achieved through a controlled process to ensure predictable structure, composition, molecular weight and material properties.

Poly(ester imide) is considered a unique material that combines the (bio)degradability and biocompatibility of polyesters with the outstanding thermal stability and mechanical properties of polyimides within the same macromolecule. Traditionally, the synthesis of poly(ester imide)s has mainly been focused on producing ester-containing dianhydrides[19–21] or diamines[22–24] for subsequent imidization polycondensation; alternatively, imide-containing diacids,[25] diols,[26,27] or their derivatives[25] are prepared for further polymerization. For example, Chen *et al.* synthesized a bio-based ester-containing diamine from isosorbide, which was then reacted with three dianhydrides to produce high-performance poly(ester imide)s for flexible electronic applications.[23] Sawada *et al.* reported isosorbide-derived ester-containing dianhydrides for the preparation of optically active semialicyclic polyimides.[21] Concerning (bio)degradable poly(ester imide)s, He *et al.* synthesized an imide dihydric alcohol from pyromellitic dianhydride and ethanolamine, and copolymerized it with succinic acid and 1,4-butanediol to produce biodegradable copolymers.[26] Su *et al.* reported a method for converting citric acid into imide-containing diacids and diesters, which were then polymerized with various linear diols to obtain water-degradable polymers.[25] Typically, reducing the costs associated with feedstocks, reaction steps, reagents, catalysts and related

[a]*School of Materials Science and Engineering, Zhejiang University, Hangzhou 310027, China*
[b]*Research Center for Industries of the Future, Westlake University, No. 600 Dunyu Road, Hangzhou 310030, Zhejiang Province, China*
[c]*School of Engineering, Westlake University, No. 600 Dunyu Road, Hangzhou 310030, Zhejiang Province, China*

† Electronic supplementary information (ESI) available. See DOI: https://doi.org/10.1039/d5py00190k

processes involved in the production of polymeric monomers and polymers with desirable material properties is essential for making these materials competitive in the current industry.

The typical synthesis routes of polyimides often involve the formation of poly(amic acid)[28–30] or poly(amic alkyl esters),[31–33] followed by thermal imidization. Inspired by the internal catalysis and neighboring group participation, it was hypothesized that the same concept could be applied to the one-pot synthesis of imide-containing polyesters. Additionally, the presence of succinimide end groups has been confirmed in the final poly(ester amide) product when dimethyl succinate is used.[34] The formation of imide intermediates during the transamidation process has been demonstrated for the first time with the hot processing of specific polyamide networks.[35] Specifically, significant advancements in polyester synthesis through a catalyst-free melt polycondensation mechanism using excess dicarboxylic acids and diols[36,37] suggested that related dicarboxylic acids are possibly available for the conversion of corresponding amic acid into imide, and their functional role in polymerization could be harnessed. Consequently, integrating the formation of imides with the synthesis of esters in a one-pot process is promising for achieving the desirable imide-containing polyesters.

In this work, we explored the opportunity for a simple one-pot synthesis of desirable poly(ester amide)s *via* the melt polycondensation of excess dicarboxylic acid with ethanolamine, which inadvertently led to the production of a novel di(ester imide) compound. This allowed us to systematically study the reaction mechanism and screen suitable substrates, leading to the development of a universal model reaction for the synthesis of di(ester imide)s (Fig. 1a). Density functional theory (DFT) calculations revealed that the autocatalysis of amic acid was crucial for imide formation, an essential step for extending the model reaction to polymer synthesis. Furthermore, we successfully synthesized a series of thermoplastic polyesters with side-chain-containing imide groups from amino diols and dicarboxylic acids using the one-pot melt polycondensation process (Fig. 1b). The most desirable transformation from amino to amide to imide proceeded completely without cross-linking during the chain propagation process. Additionally, 1,4-butanediol was introduced to produce a family of copolymers (Fig. 1c). The material properties of the synthesized polyester with side-chain-containing imide group were investigated, encompassing (bio)degradable semicrystalline or amorphous polymers with a wide range of glass transition temperature (T_g) values, broad mechanical properties, and straightforward processability. The one-pot synthesis for linear imide-containing polyesters has been demonstrated to be structurally versatile, programmable, and universal.

2. Experimental section

Experimental materials, general methods, and experimental details are all described in the ESI.†

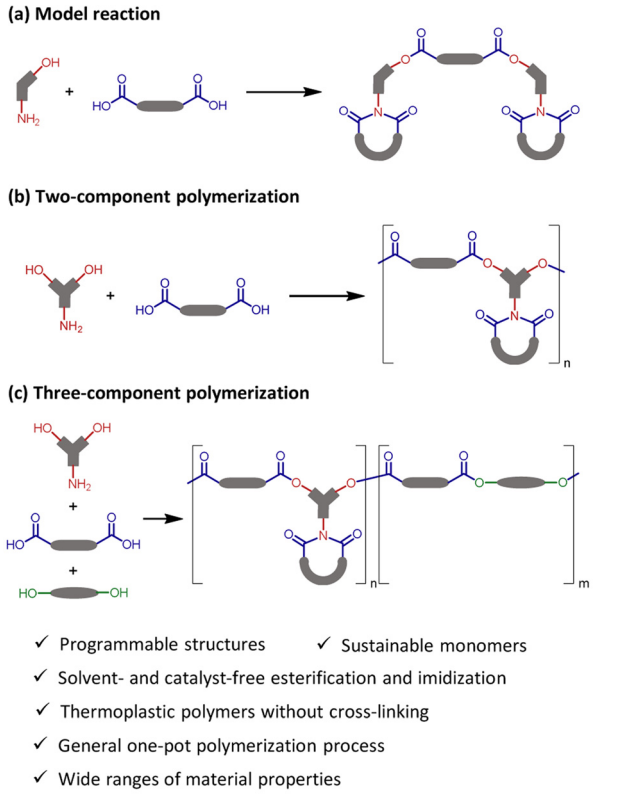

Fig. 1 (a) Model reaction for the synthesis of the di(ester imide) compound. (b) Model-inspired two-component polymerization for the synthesis of the imide-containing polyester. (c) Model-inspired three-component polymerization for the synthesis of the imide-containing polyester.

3. Results and discussion

3.1 Model reaction

It was originally hypothesized that a mechanically tough and strong poly(ester amide) could be synthesized via heat-promoted amidation, esterification and re-esterification from amino alcohol and dicarboxylic acid. In an initial attempt, succinic acid and 2-aminoethanol, used as starting materials, were reacted in a set molar ratio of 1.1 : 1 through a one-pot, two-step procedure (Fig. S1,† entry 1). However, an insoluble solid product was unexpectedly obtained. Characterization by nuclear magnetic resonance (NMR) spectroscopy (Fig. S6 and S7†) and high-resolution mass spectrometry (HRMS) indicated its unique structure containing two ester and two imide groups, namely di(ester imide) **DI-1**. With an increasing feed of succinic acid, excellent yields of the di(ester imide) were achieved (Fig. S1†).

To confirm whether similar di(ester imide) compounds could also be synthesized, we explored other potential amino alcohols, such as DL-alaninol and DL-1-amino-2-propanol, along with various dicarboxylic acids (Fig. 2b). These included substituted succinic acids like 2-methylsuccinic acid (**2b**), 2,2-dimethylsuccinic acid (**2c**), 2-phenylsuccinic acid (**2d**), phthalic acid (**2e**), cyclohexane-1,2-dicarboxylic acid (**2f**), and long

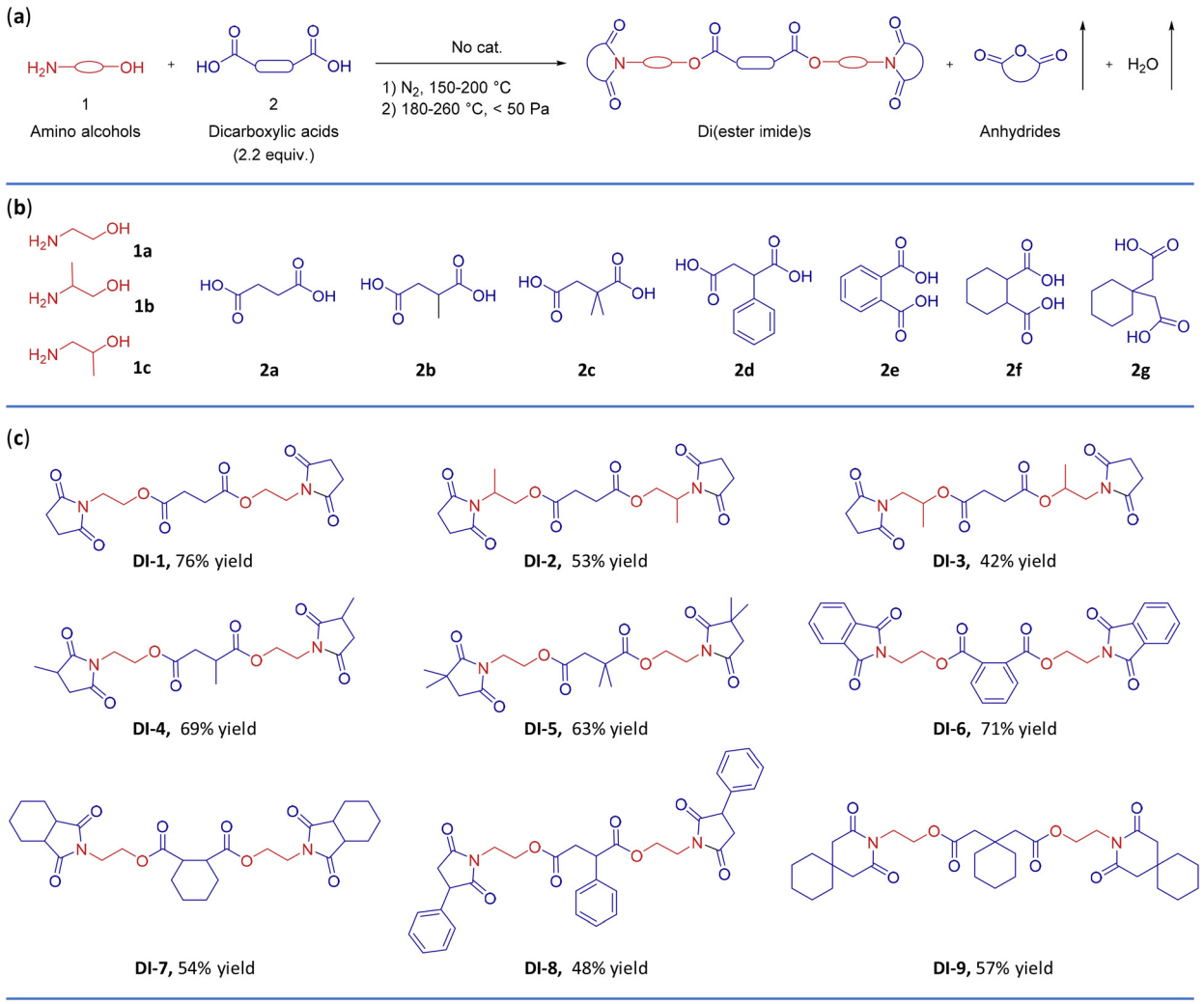

Fig. 2 Substrate scope for the model reaction. (a) Synthetic route. (b) Alternative substrates that include three amino alcohols and seven dicarboxylic acids. (c) The nine obtained di(ester imide) products.

carbon-chain dibasic acids, such as glutaric acid, adipic acid and 1,1-cyclohexanediaceticacid (**2g**), which can form five-, six- or seven-membered cyclic anhydrides and potential cyclic imides. Experimental results indicated that these related di(ester imide) compounds, from **DI-2** to **DI-9**, were synthesized with good yields (Fig. 2c). Their structures were confirmed by ^{1}H NMR, ^{13}C NMR (Fig. S8–S23†) and HRMS. However, the lower ring tension effect may have impeded the formation of anhydride or cyclic imide, resulting in the inability to synthesize di(ester imide) from glutaric acid and adipic acid, respectively.

Building on these successful results, we further investigated the potential reaction mechanism for the synthesis of di(ester imide) from the corresponding amino alcohol and excess dicarboxylic acid. Notably, under solvent- and catalyst-free conditions, the reaction process of 2-aminoethanol and succinic acid (2.0 equiv.) was monitored by ^{1}H-NMR (Fig. S2†). The proton signal of the methylene group on the succinimide ring was located at 2.62 ppm. Triplet peaks at 3.60 ppm and 4.13 ppm represented the corresponding proton signals of the methylene group between the nitrogen atom of succinimide and the oxygen atom of the ester. Upon continuous heating and nitrogen purging, proton signals at 2.62 ppm, 3.60 ppm and 4.13 ppm appeared, providing clear evidence of the formation of ester and succinimide, resulting in the target molecule **DI-1**. Potential compounds involved in this reaction process were further confirmed by HRMS (Fig. S4†), with key compounds listed in Table S1.† The reaction by-products removed were observed as water vapor and a white solid (Fig. S1†), identified as succinic anhydride (Fig. S3†). These phenomena are consistent with the literature, which reports that high molecular weight polyesters can be produced by a tandem mechanism involving the removal of by-products, such as water and succinic anhydride.[36] Combining these encouraging results, we propose the following reaction routes for the synthesis of **DI-1** (Fig. S5†), which involve amidation,

esterification, re-esterification, imidization, and the reported tandem mechanism.[36] These pathways are generally applicable to the synthesis of other di(ester imide)s.

3.2 Mechanism study on the autocatalysis of amic acid

The formation of imides through the autocatalysis of amic acid is a significant process in the development of imide-containing small molecules or polymers. DFT calculations of the free energy difference ($\Delta G^{\ddagger}$) were performed to elucidate how amic acid structures and substituents influence the selectivity in imide formation (Fig. 3a). Four typical examples of the calculation results include $\mathbf{I_{2a}}$, $\mathbf{I_{2e}}$, $\mathbf{I_{2f}}$ and $\mathbf{I_{2g}}$, with their free energy differences at the transition state (TS) ranging from 194.02 to 268.30 kcal mol^{-1} (Fig. 3b). This variation is closely

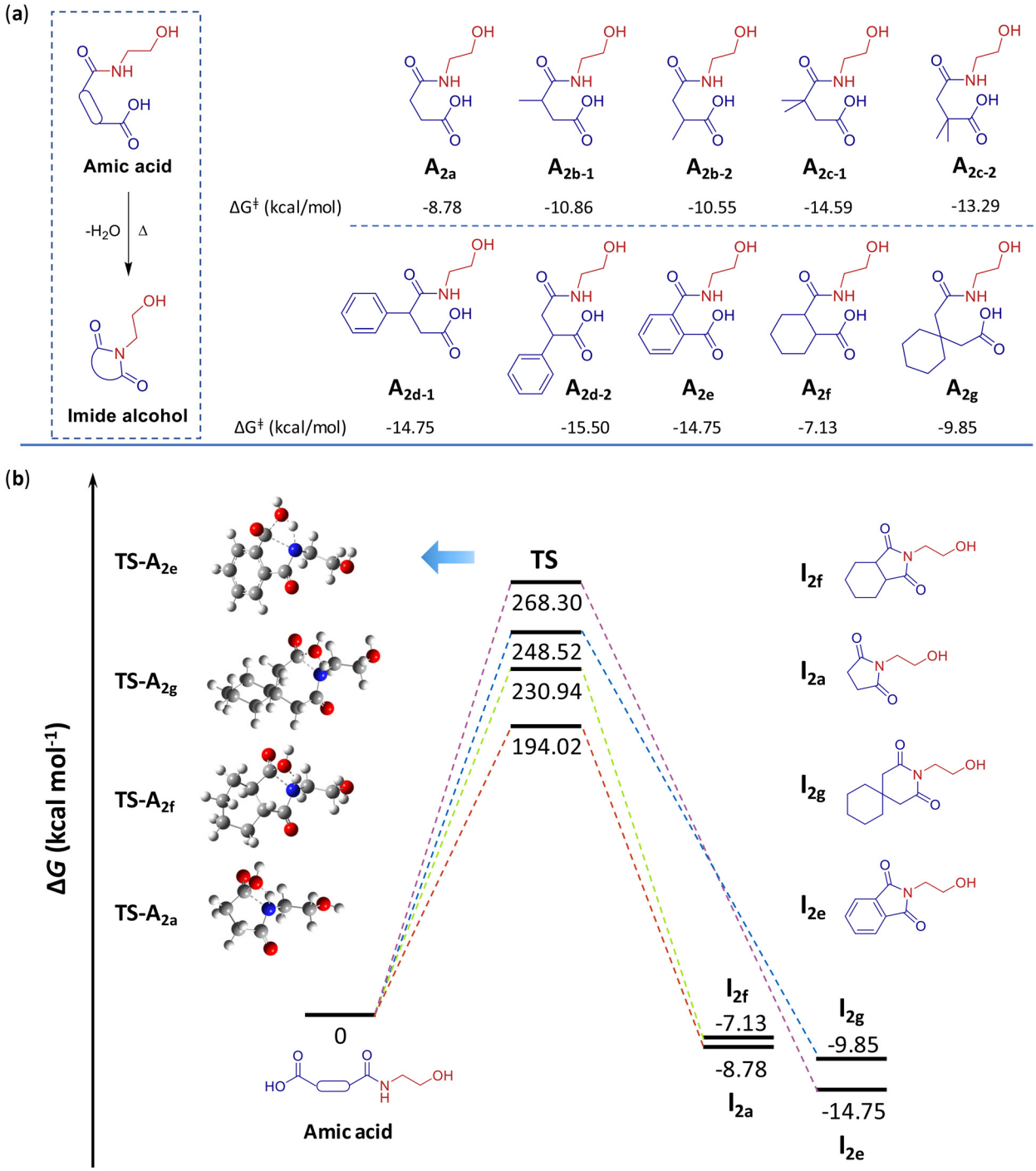

Fig. 3 DFT calculations for imidization. (a) Free energy values associated with the thermal imidization process of amic acid. (b) DFT-calculated energy profiles for the formation of imides from four typical amino acids.

linked with the ring strain of the corresponding amic acid, decreasing in the order **TS-A$_{2e}$**, **TS-A$_{2g}$**, and **TS-A$_{2f}$**, indicating a gradual reduction in ring strain. For succinic acid-derived amic acids, the same substituent at different locations exhibited similar free energy differences at the TS (Fig. S24–S26†). However, as the substituent changed from methyl to dimethyl to phenyl, the corresponding free energy differences at the TS values gradually increased, likely due to increased substituent site resistance. Comparing with the reported formation of cyclic anhydrides,[36] the higher energy state associated with the activation of amic acid makes it the rate-limiting step, consistent with the observation that actual experiments require extended durations. Moreover, the theoretical heat of imidization values were calculated to be significantly negative, ranging from −15.50 to −7.13 kcal mol^{-1} (Fig. 3a), suggesting that the process is thermodynamically highly favorable.

3.3 Model-inspired two-component polymerization

Encouraging model reaction results facilitated the identification of viable dicarboxylic acids and elucidation of the corresponding imide formation mechanism. The typical process of removing water and anhydride to promote molecular propagation in the model reaction can be extended to produce imide-containing polyester when amino diols and dicarboxylic acids are used as starting materials. In an initial attempt, a reaction with a feeding ratio of succinic acid (**2a**)/3-amino-1,2-propanediol (**3a**) of 2.1 : 1 conducted under melt and continued nitrogen flow conditions (Fig. 4a) achieved full conversion from amino to amide to imide within 12 h (monitored by ^{1}H NMR) (Fig. 4c and d). Subsequent application of a vacuum (<50 Pa) to distil the reaction by-products and drive polycondensation yielded a transparent polymer, designated P(**2a3a**) (Fig. 4b). The chemical structure of succinimide-containing polyesters was confirmed by FTIR spectra (Fig. S27†) and NMR spectra (Fig. S28–S31†). Gel permeation chromatography (GPC) characterization of P(**2a3a**) revealed a sharp and symmetrical peak with a number-average molecular weight (M_n) of 4.2 kDa (Fig. S32a†). Further thermal and crystalline analysis indicated that P(**2a3a**) is amorphous, thermoplastic and thermally stable, with a high glass transition temperature (T_g = 68.5 °C) and decomposition temperature at 5% weight loss (T_{d5} = 333 °C) (Fig. S32b–d†). Despite the potential for **3a** to serve as a cross-linking point due to its trifunctional nature, experimental results demonstrated that all amino groups of **3a** were successfully converted into side-chain succinimide groups, resulting in a linear, thermoplastic polyester with side-chain-containing succinimide groups without cross-linking.

To synthesize imide-containing polyesters with high molecular weight, polycondensation times of 24 h and 48 h were employed (Table 1, entries 2 and 3). Likely because of the high

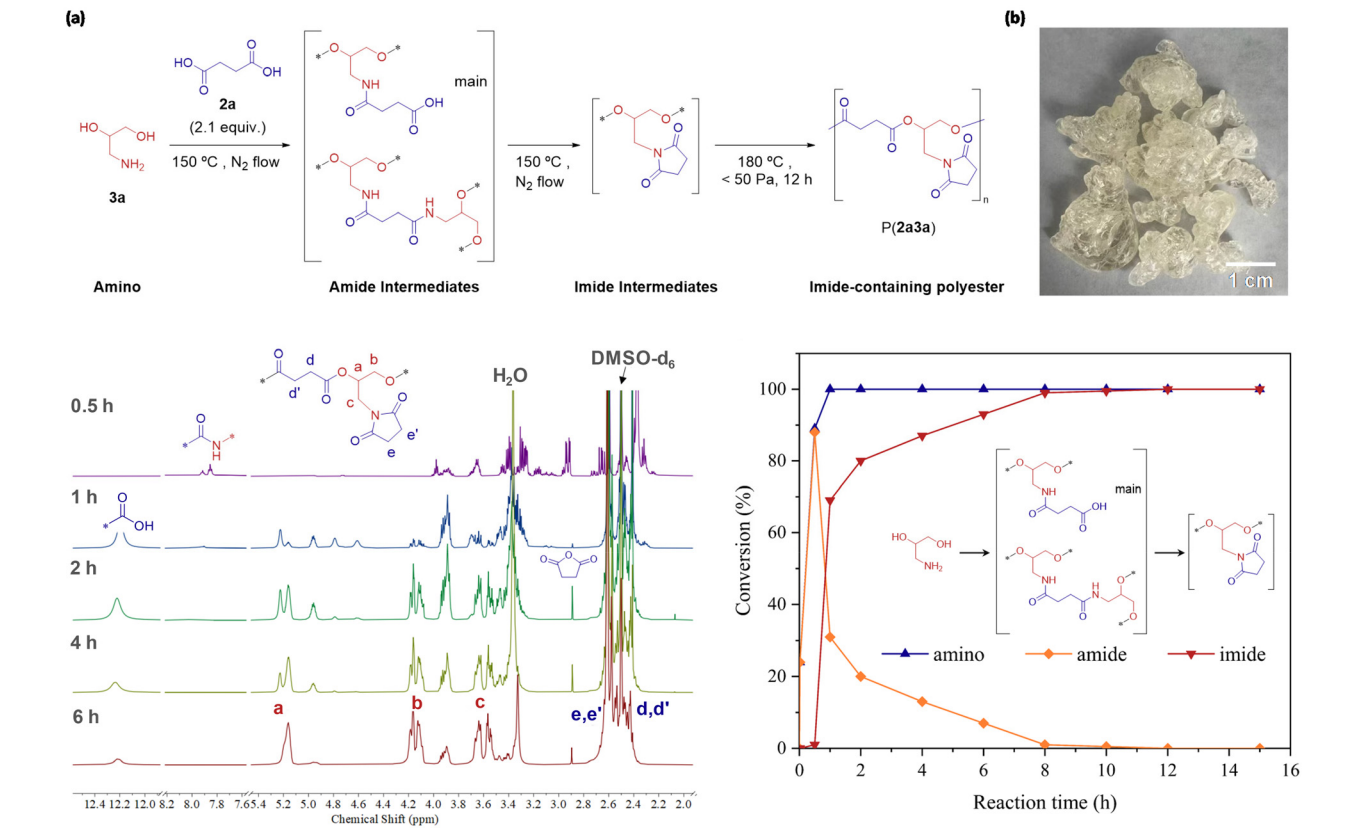

Fig. 4 One-pot synthesis of imide-containing polyester P(**2a3a**) *via* conventional melt polycondensation. (a) Proposed reaction pathways. (b) Photograph of P(**2a3a**) as a transparent bulk solid. (c) Stacked ^{1}H NMR spectra of the reaction mixture at various time points. (d) Conversion kinetics from amino (**3a**) to amide to imide, quantified based on ^{1}H NMR data.

Table 1 One-pot synthesis of P(**2a3a**) under different catalytic conditions[a]

Entry	Catalyst[b]	Time[c] (h)	M_n[d] (Da)	M_w[d] (Da)	$Đ$[d]	T_g[e] (°C)
1	—	12	4208	8079	1.92	68.5
2	—	24	5673	9081	1.60	71.6
3	—	48	6473	10 982	1.70	73.2
4	TBT	18	6241	10 360	1.66	74.5
5	$Ce(CF_3SO_4)_3$	18	7440	13 020	1.75	76.2
6	$Sc(CF_3SO_4)_3$	18	8708	15 020	1.72	78.0
7	$SnCl_2$	18	9857	17 377	1.76	77.7
8	Sb_2O_3	18	9195	16 282	1.77	77.0

[a] Reactions were carried out in a two-step polymerization process. In the first step, imidization and prepolymerization (~20 h) occurred at 150 °C under a nitrogen flow. In the second step, the temperature was increased to 180 °C, and a high vacuum (<50 Pa) was applied. [b] At the beginning of the second stage, no catalyst or 300 ppm catalyst was added. [c] Reaction time in the second stage. [d] Determined by GPC using PS standards. [e] Determined by DSC at 10 °C min^{-1}.

melt viscosity and significant steric hindrance, prolonging the polycondensation time resulted in only a minor increase in molecular weight. Subsequently, various catalysts were investigated, including titanium(IV) butoxide (TBT), stannous chloride ($SnCl_2$), cerium(III) trifluoromethanesulfonate ($Ce(CF_3SO_4)_3$), scandium(III) trifluoromethanesulfonate ($Sc(CF_3SO_4)_3$), and antimony(III) oxide (Sb_2O_3) (Table 1, entries 4–8). Analysis of their GPC curves indicated that $SnCl_2$ provided the highest M_n of 9.9 kDa (Fig. S33a† and Table 1), demonstrating its superior catalytic effect. Furthermore, the use of $SnCl_2$ produced a slightly yellow P(**2a3a**) with a high T_g (77.7 °C) (Fig. S33c† and Table 1). The same reaction system was extended to a variety of amino diol substrates, including 2-aminopropane-1,3-diol (**3b**), 2-aminobutane-1,3-diol (**3c**) and 2-amino-2-methyl-1,3-propanediol (**3d**). Corresponding imide-containing polyesters were successfully synthesized (Fig. 5b). The structures of P(**2a3b**), P(**2a3c**) and P(**2a3d**) were confirmed by NMR (Fig. S34–S39†). P(**2a3b**) exhibited a high M_n of 11.8 kDa (Table S2,† entry 3). The strong structural rigidity of polymers derived from methyl-substituted amino diols resulted in P(**2a3a**) and P(**2a3c**) showing higher T_g values compared to P(**2a3b**) and P(**2a3d**) (Fig. S40c†).

Next, the possibility of using other dicarboxylic acids (**2b–2g**) in the synthesis system was explored (Table S2,† entries 6–11). ^1H and ^{13}C NMR spectra confirmed the structure of corresponding imide-containing polyesters (Fig. S41–S52†). GPC analysis showed that using cyclohexane-1,2-dicarboxylic acid (**2f**) resulted in a high M_w of 51.9 kDa (Fig. 5b). Thermal and crystalline analysis indicated that all polymers were amorphous, and most were thermally stable with high T_{d5} values (319–379 °C), except for P(**2a3d**) (T_{d5} = 263 °C) (Table S2†). However, P(**2c3b**) could not be synthesized with high molecular weight, likely due to the rapid formation and removal of the by-product 2,2-dimethylsuccinic anhydride, which has a lower boiling point. In contrast, P(**2e3b**) also showed low molecular weight because the by-product phthalic anhydride, with a higher boiling point, was more difficult to remove.

Notably, the series of imide-containing polyesters (Fig. 5b) exhibited well-defined components with M_w values ranging from 3.4 to 51.9 kDa and a wide range of T_g values from 33.5 °C to 115.4 °C (Fig. 5c). These results demonstrate the synthesis flexibility of imide-containing polyesters, which can be tailored using various amino diols and dicarboxylic acids. The steric hindrance effects of the hydroxyl groups in the amino diol, and the anhydride formation performance play a crucial role in the polycondensation process, thereby influencing the molecular weight of the imide-containing polyesters. Future work aims to identify new monomers and effective strategies to produce high molecular weight imide-containing polyesters.

3.4 Model-inspired three-component polymerization

Previous studies on the one-pot synthesis of the two-component system have shown that hydroxyl groups have no influence on the imidization process. Moreover, the potential for polymer cross-linking due to a possible reaction between the carboxyl group of the amic acid and the hydroxyl group has been excluded. Consequently, we investigated the possibility of introducing another diol. 1,4-Butanediol (**4a**) is a significant chemical commonly used in the plastics industry to produce polymers such as poly(tetrahydrofuran), poly(butylene succinate) (PBS), poly (butylene succinate-*co*-terephthalate) (PBST), and poly(butylene adipate-*co*-terephthalate) (PBAT), as well as other polymers.[38–42] On introducing **4a** into the synthetic system to react with **2a** and **3a** (Fig. 6a), the mixture was heated to 150 °C under nitrogen flow to transform the amino group into the succinimide group and prepare prepolymers within 20 h. Subsequently, a polycondensation catalyst, $SnCl_2$, was added. The reaction was then heated to 220 °C, and a vacuum of less than 50 Pa was slowly applied to distil the water and succinic anhydride by-products, thereby driving the polycondensation reaction for approximately 24 h. By controlling the feed ratio of **3a**/**4a**/**2a**, we theoretically obtained well-defined copolymers, denoted as P(**2a3a4a**)$_x$ (where x is the percentage of **3a** in all diols) (Table S3†). The block content of the copolymers is x, which also indicates the content of P(**2a3a**) (imide-containing block). In addition, we successfully synthesized P(**2a3b4a**)$_{15}$, P(**2a3c4a**)$_{15}$ and P(**2a3d4a**)$_{15}$ (Fig. 6b) by controlling the molar proportion of amino diols (**3b–3d**) to 15% among all diols. P(**3d3b4a**)$_{30}$, P(**3e3b4a**)$_{30}$, P(**3f3b4a**)$_{30}$ and P(**3g3b4a**)$_{30}$ (Fig. 6b) were also produced using similar strategies, starting from dicarboxylic acids (**2d–2g**), 2-aminopropane-1,3-diol (**3b**) and 1,4-butanediol (**4a**).

FTIR characterization was performed on the resulting copolymers (Fig. S55–S58†). For example, P(**2a3a4a**)$_{70}$ revealed absorption peaks at 1728 and 1695 cm^{-1} that correspond to the stretching vibrations of C=O in succinimide and succinate ester groups, respectively, while peaks at 1400 and 1146 cm^{-1} correspond to the stretching vibrations of C–N and C–O, respectively. As the succinimide content increased, the absorption intensity of the C=O and C–N stretching vibrations was commonly enhanced, and the absorption intensity of the C–O stretching vibration gradually weakened due to the decreased succinate ester content (Fig. S55†).

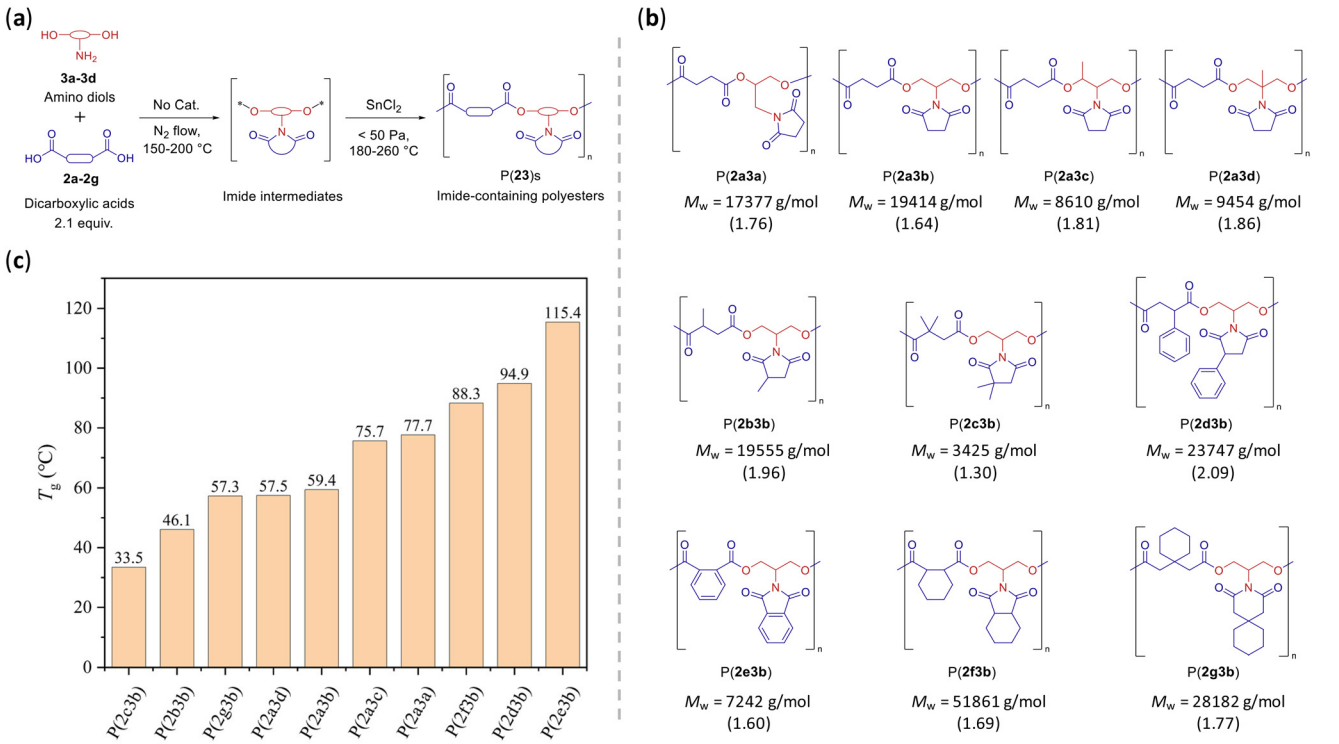

Fig. 5 One-pot synthesis of imide-containing polyesters from two-component starting materials. (a) Proposed reaction pathways. (b) The series of produced imide-containing polyesters and corresponding molecular data. (c) T_g values of the imide-containing polyesters.

The chemical structures of copolymers were further analyzed by ^{1}H NMR and ^{13}C NMR spectroscopy (Fig. S59–S84†). For the series of P(**2a3a4a**)$_x$ copolymers, characteristic peak signals of the tertiary carbon protons in the copolymers were observed at 5.29 ppm (b in Fig. S59†). Multiple characteristic peak signals at 3.86–3.55 and 3.76–3.65 ppm (d and e in Fig. S59†) correspond to the methylene protons adjacent to the nitrogen atom and succinimide, respectively. No amide proton linkage signals were observed at 8.50–7.50 ppm, indicating that the amino groups of **3a** were fully converted into succinimide groups, confirming the full imidization by amic acid. As the feed of **4a** decreased, characteristic peak signals of the methylene groups in the copolymers were observed at 4.07 and 1.67 ppm (f and g in Fig. S59†), corresponding to 1,4-butanediol. The intensity of these characteristic peak signals varied in response to changes in the content of the P(**2a3a**) block and the PBS block. The corresponding ^{13}C NMR spectrum also confirmed the correctness of the structure. The other series of copolymers with 15% and 30% molar ratios of the imide-containing block exhibit a close correspondence with nuclear magnetic resonance (NMR) structures. These results suggest that the copolymers possess a well-defined structural unit, and their composition can be precisely controlled by adjusting the feed ratio.

3.5 Properties of imide-containing copolymers

GPC characterization of various P(**2a3a4a**)$_x$ copolymers revealed a broad M_n range from 10.5 kDa to 45.0 kDa, with narrow dispersity ($Đ$) values below 2.18 (Fig. S85† and Table S3†). Notably, P(**2a3a4a**)$_{2.5}$, synthesized with a **3a**/**4a**/**2a** feed ratio of 0.025/0.975/1.125, exhibited a high M_n of 45.0 kDa and a narrow $Đ$ of 1.46. Increasing the **3a**/**4a**/**2a** feed ratio to 0.90/0.10/2.00 resulted in a low M_n (10.5 kDa) due to the strong steric effect of the succinimide-containing diol. P(**2a3a4a**)$_x$ materials exhibited thermal stability, with high T_{d5} values ranging from 342 to 366 °C (Fig. S88a, b and Table S3†), consistent with PBS and P(**2a3a**). As the hard content of P(**2a3a**) increased, the crystallinity of the copolymers decreased from 70.1% to 0% (Table S3†). PBS is a semicrystalline, biodegradable polymer with a melting temperature (T_m) of 114–116 °C and an equilibrium melting temperature in the range of 127.5–146.5 °C.[40] Copolymers with hard content values of P(**2a3a**) less than 20% exhibited crystalline properties and low glass transition temperature values (T_g = −24.6 to −8.5 °C), along with high melting transition temperature (T_m = 89.4 to 114.9 °C) and crystalline transition temperature (T_c = 51.8 to 69.6 °C) values (Fig. 7a and Table S3†). Copolymers with hard content values of P(**2a3a**) ranging from 20% to 90% exhibited high glass transition temperature values (T_g = −14.2 to 56.2 °C) (Fig. S88d and Table S3†). The T_g values of P(**2a3a4a**)$_x$, as determined by DSC, did not exhibit a regular trend (Fig. 7c). Conversely, DMA characterization revealed that the T_g values of the copolymers increased with higher P(**2a3a**) content (Fig. S89–S91†). Further examination by wide-angle X-ray scattering (WAXS) showed that P(**2a3a4b**)$_x$ (x = 2.5 to 30) yielded four characteristic diffraction bands at 19.8, 22.0, 22.8

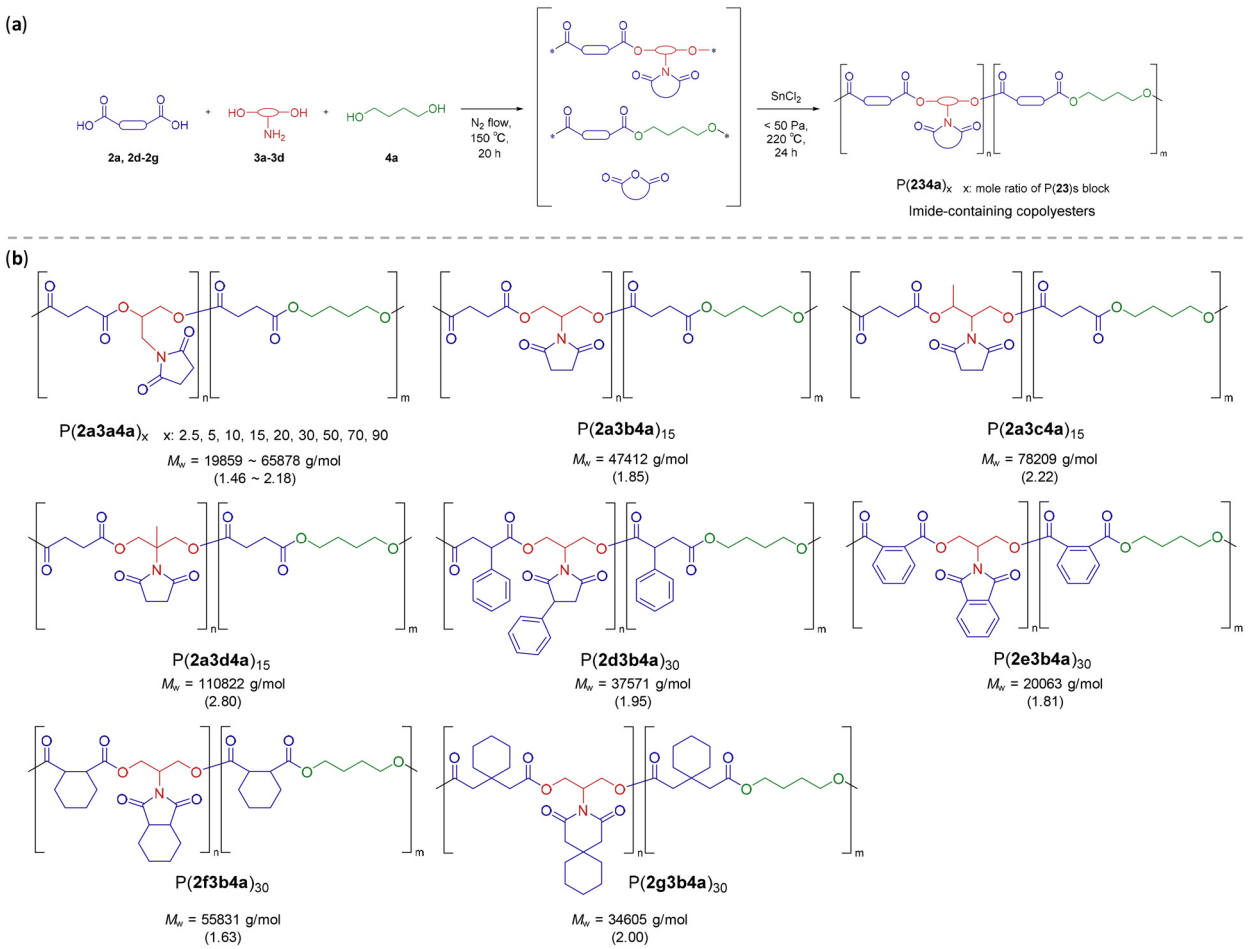

Fig. 6 One-pot synthesis of imide-containing copolyesters from three-component starting materials. (a) Proposed reaction pathways. (b) The series of produced imide-containing copolyesters and corresponding molecular data.

and 29.2° (Fig. S91†), similar to those of PBS copolymers.[38,40] These bands are assigned to the (020), (021), (110) and (111) planes, respectively.[43–45] Although the crystalline transition temperature (T_c) of P(**2a3a4a**)$_{20}$ and P(**2a3a4a**)$_{30}$ was not observed during the first cooling scan for DSC, the characteristic diffraction bands of P(**2a3a4a**)$_{20}$ and P(**2a3a4a**)$_{30}$ indicate the presence of crystallinity, likely due to their low crystallinity and crystallization rate.

Copolymers with a 15% molar ratio of the imide-containing block, such as P(**2a3a4a**)$_{15}$, P(**2a3b4a**)$_{15}$, P(**2a3c4a**)$_{15}$ and P(**2a3d4a**)$_{15}$, are semicrystalline elastic polymers with T_m near 100 °C (Fig. 7b and Table S4†), T_g below −20 °C (Fig. 7c and Table S4†), and crystallinity ranging from of 26.9% to 51.1% (Table S4†). Notably, P(**2a3b4a**)$_{15}$ exhibited a high crystallinity of 51.1% because of the high structural processibility contributed by 2-aminopropane-1,3-diol (**3b**). Copolymers with a 30% molar ratio of imide-containing block including P(**2d3b4a**)$_{30}$, P(**2e3b4a**)$_{30}$, P(**2f3b4a**)$_{30}$ and P(**2g3b4a**)$_{30}$, are amorphous polymers with T_g values ranging from −3.9 °C to 37.4 °C (Fig. 7c and Fig. S95b, Table S4†). Theoretically, any imide-containing polymer with a T_g value from −25 °C to 115 °C can be synthesized by changing the feed of **3a–3d**/**2a–2g**/**4a**. These results indicate that we could design the desirable polymer with programmable structures and thermal properties.

The mechanical properties of the copolymers were investigated *via* uniaxial tensile testing using dumbbell-shaped samples (Fig. S97–S105†). As the hard content of P(**2a3a**) increased, the copolymer properties transitioned from brittle to strong and then back to brittle. The average ultimate tensile strength (σ_{UTS}) decreased from 34.5 MPa for P(**2a3a4a**)$_{2.5}$ to 8.0 MPa for P(**2a3a4a**)$_{30}$. Notably, P(**2a3a4a**)$_5$ and P(**2a3a4a**)$_{10}$ exhibited mechanically tough and strong properties, with σ_{UTS} values of 21 and 22 MPa, respectively, and average elongations at break (ε) values of 107% and 325%, respectively (Fig. 7d and Table S5†). Comparing the imide-containing block at a 15% molar ratio in various copolymers, these materials exhibited mechanically tough and strong properties, with σ_{UTS} up to 23.7 MPa and maximum ε of 472% (Fig. 7e and Table S6†). These materials demonstrated competitive or superior mechanical

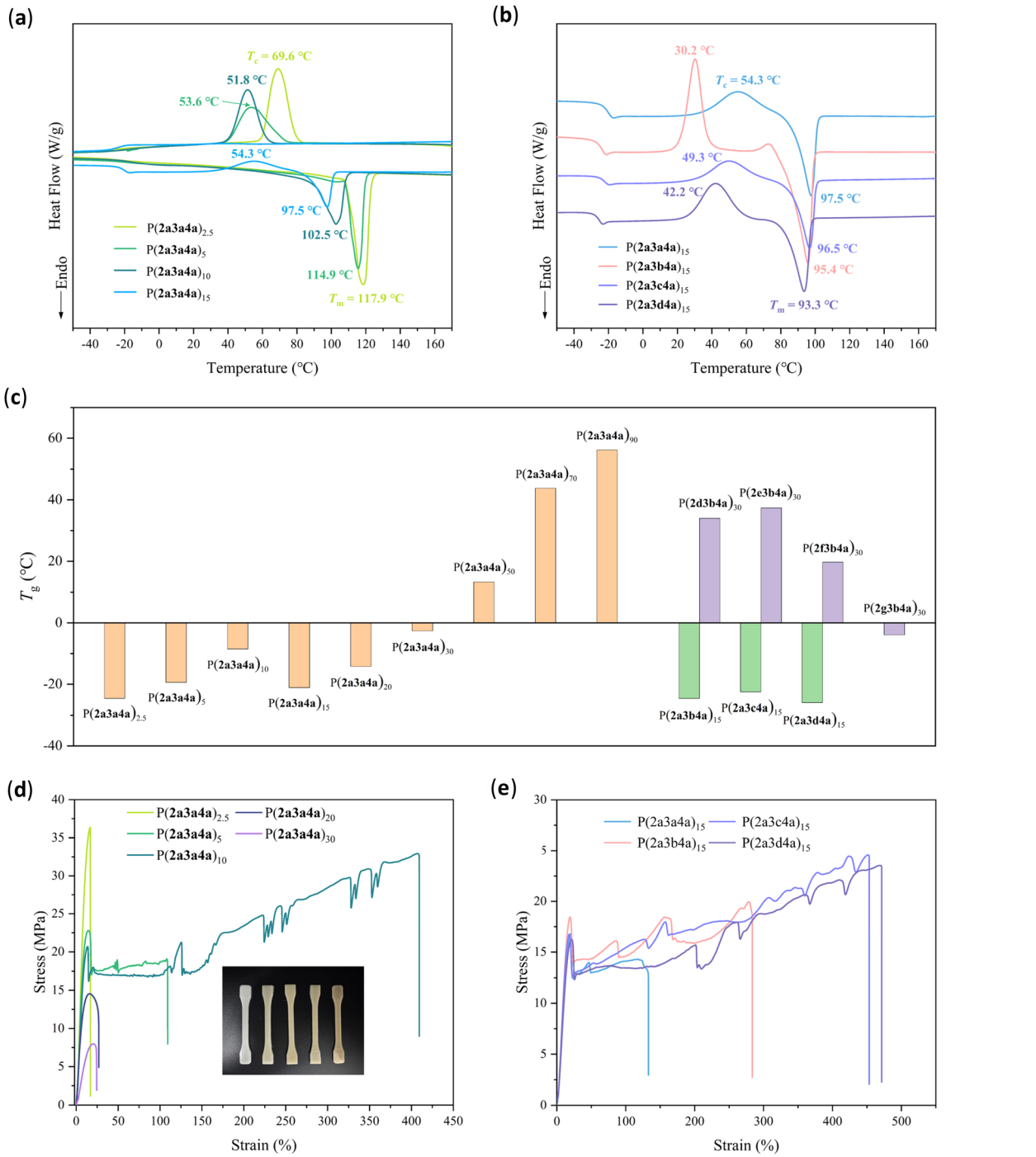

Fig. 7 Thermal and mechanical properties of the obtained copolymers. (a) DSC curves of P(**2a3a4a**)$_x$, x = 2.5, 5, 10, and 15. (b) DSC curves of P(**2a3a4a**)$_{15}$, P(**2a3b4a**)$_{15}$, P(**2a3c4a**)$_{15}$ and P(**2a3d4a**)$_{15}$. (c) T_g values of the obtained copolymers. (d) The stress–strain curves of P(**2a3a4a**)$_x$, x = 2.5, 5, 10, 20 and 30. The inset photograph shows the dumbbell-shaped samples. (e) The stress–strain curves of P(**2a3a4a**)$_{15}$, P(**2a3b4a**)$_{15}$, P(**2a3c4a**)$_{15}$ and P(**2a3d4a**)$_{15}$.

properties compared to those of petroleum-based high-density polyethylene (HDPE), low-density polyethylene (LDPE) and polypropylene (PP).

Furthermore, P(**2a3a4a**)$_{10}$, P(**2a3b4a**)$_{15}$, P(**2a3c4a**)$_{15}$ and P(**2a3d4a**)$_{15}$ exhibited excellent biodegradability (near 86% on day 180) (Fig. 8a and c). Among these, P(**2a3c4a**)$_{15}$ and P(**2a3d4a**)$_{15}$ showed a similar trend in cellulose degradation compared to the reference material. In the first 80 days, a relatively rapid degradation rate was observed, with the biodegradation rate approaching 78%. Subsequently, the trend leveled off, with less than 10% additional degradation over the remaining 100 days. Conversely, P(**2a3a4a**)$_{10}$ and P(**2a3b4a**)$_{15}$

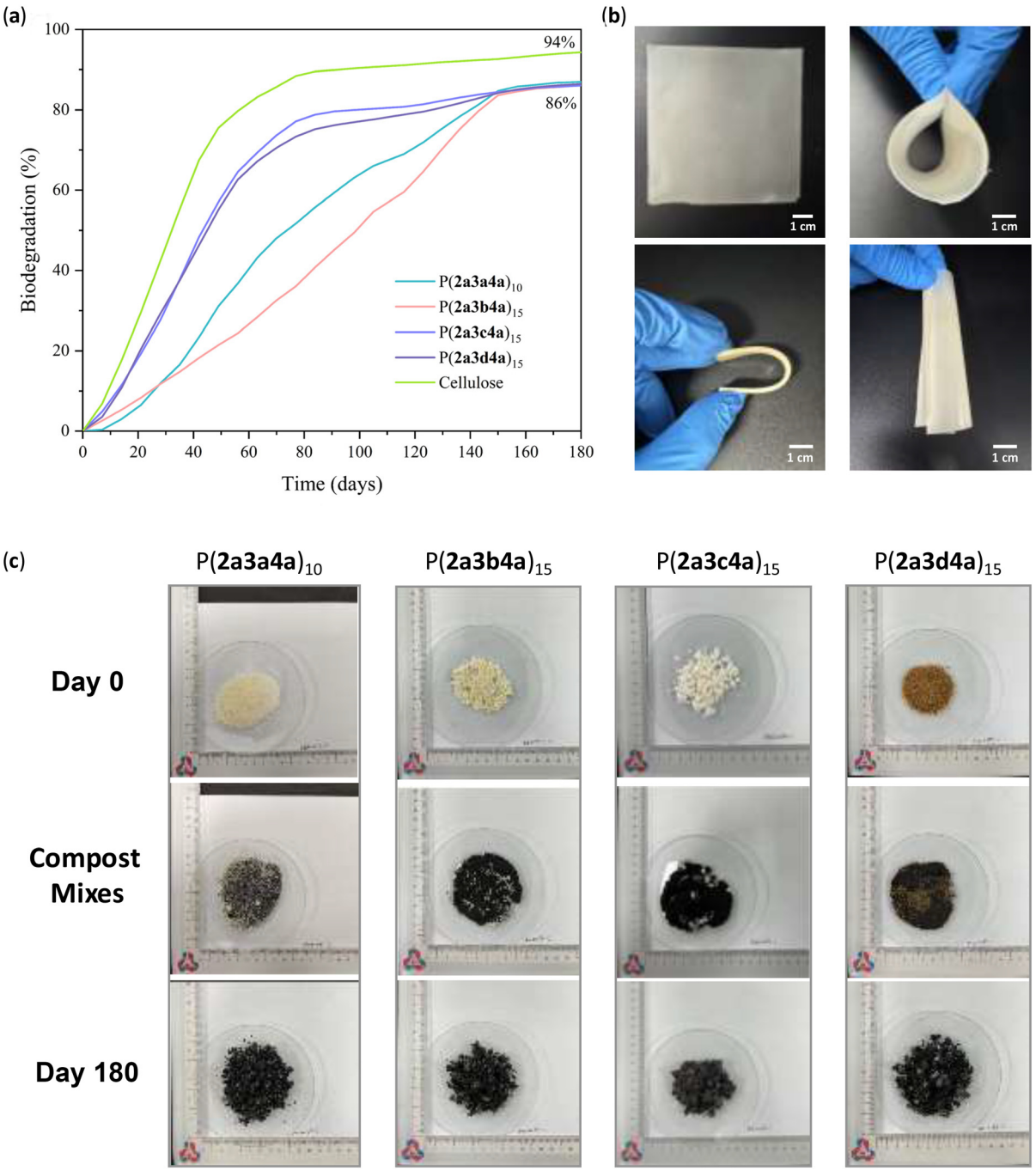

Fig. 8 Illustration of the biodegradability of copolymers. (a) Experiment day *versus* biodegradation. (b) Photograph of a dumbbell-shaped specimen of P(**2a3a4a**)$_{10}$ under bending; photographs of a hot-pressed film (10 cm × 10 cm × 208 μm) and the film under bending. (c) Photographs from the composting degradation experiment for four polymers.

exhibited a stable biodegradation rate over the first 150 days, with the rate curve remaining nearly linear over time. These polymers also demonstrated excellent straightforward processability, including hot-press and melt spinning (Fig. 8b). As biobased, biodegradable and high-performance polymers, these materials are promising and could be widely used for shelf-life products, including sustainable fibers, packaging and mulch films.

4. Conclusions

This paper reports a novel synthetic methodology for polyesters with side-chain-containing imide groups, derived from two-component amino diol/dicarboxylic acid or three component amino diol/diol/dicarboxylic acid systems. This method was inspired by the reaction of an amino alcohol and excess dicarboxylic acid to form small-molecular di(ester

imide) compounds through traditional melt condensation. Extensive substrate investigations led to the development of a general and accessible model reaction for the condensation of amino alcohol and excess dicarboxylic acid. DFT calculations and experimental studies elucidated the dual role of dicarboxylic acid in imidization, esterification, re-esterification, and chain propagation during melt condensation. This synthetic system was extended to the polymerization of amino diols and dicarboxylic acids, wherein the amino groups of amino diols were fully transformed into the imide groups *via* amic acid imidization, without causing polymer cross-linking. A variety of amino diols and dicarboxylic acids were employed to synthesize a series of thermoplastic imide-containing polyesters with aliphatic or aromatic structures. Most of these imide-containing polyesters exhibited high thermal stability and a broad range of T_g values from 33.5 to 115.4 °C. To expand the structural diversity of imide-containing polyesters, 1,4-butanediol was introduced into the synthetic system. The polymerization of 3-amino-1,2-propanediol, 1,4-butanediol and succinic acid yielded a family of imide-containing copolyesters with well-defined structures and tunable properties. The PBS copolymer for the imide-containing block at 15% molar ratio exhibits excellent mechanical properties. Programmable structures and controllable properties could be achieved by altering the starting materials and feed ratio. This work significantly advances the fundamental study of integrating multiple material chemistries to develop polymers with enhanced performance characteristics.

Data availability

Data are available within the article or its ESI.†

Conflicts of interest

The authors declare that they have competing financial interests. K. Z. and T. R. have filed a patent application on this technology.

Acknowledgements

This work was supported by the Missa Ice City Foundation, the Muyuan Foundation and the Westlake Education Foundation. We thank Dr Yinjuan Chen, Dr Zhong Chen, Xiaohuo Shi, Cuili Wang and Danyu Gu from the Instrumentation and Service Center for Molecular Sciences and Dr Xiaohe Miao, Dr Ying Nie, and Dr Zhen Yang from the Instrumentation and Service Center for Physical Science at Westlake University for their technical assistance in obtaining the measurements.

References

1 F. S. Bates, M. A. Hillmyer, T. P. Lodge, C. M. Bates, K. T. Delaney and G. H. Fredrickson, *Science*, 2012, **336**, 434–440.
2 C. M. Bates and F. S. Bates, *Macromolecules*, 2017, **50**, 3–22.
3 J. M. Eagan, J. Xu, R. Di Girolamo, C. M. Thurber, C. W. Macosko, A. M. LaPointe, F. S. Bates and G. W. Coates, *Science*, 2017, **355**, 814–816.
4 J. Xu, X. Wang and N. Hadjichristidis, *Nat. Commun.*, 2021, **12**, 7124.
5 M. Xiong, D. K. Schneiderman, F. S. Bates, M. A. Hillmyer and K. Zhang, *Proc. Natl. Acad. Sci. U. S. A.*, 2014, **111**, 8357–8362.
6 D. K. Schneiderman, M. E. Vanderlaan, A. M. Mannion, T. R. Panthani, D. C. Batiste, J. Z. Wang, F. S. Bates, C. W. Macosko and M. A. Hillmyer, *ACS Macro Lett.*, 2016, **5**, 515–518.
7 M. S. Meyersohn, A. Block, F. S. Bates and M. A. Hillmyer, *Macromolecules*, 2024, **57**, 9230–9240.
8 Y. Wang and S. M. Grayson, *Adv. Drug Delivery Rev.*, 2012, **64**, 852–865.
9 Y. Li, T. Thambi and D. S. Lee, *Adv. Healthcare Mater.*, 2018, **7**, 1700886.
10 A. A. Assiri, K. Glover, D. Mishra, D. Waite, L. K. Vora and R. R. S. Thakur, *Drug Discovery Today*, 2024, **29**, 104098.
11 R. D. Cheng, M. W. Xu, X. H. Zhang, J. Q. Jiang, Q. Y. Zhang and Y. Zhao, *Angew. Chem., Int. Ed.*, 2023, **62**, e202302900.
12 K.-H. Wang, C.-H. Liu, D.-H. Tan, M.-P. Nieh and W.-F. Su, *ACS Appl. Mater. Interfaces*, 2024, **16**, 6674–6686.
13 M. Radjabian and V. Abetz, *Prog. Polym. Sci.*, 2020, **102**, 101219.
14 S. Y. Lee, D. R. Kang, J.-G. Oh, I. S. Chae and J. H. Kim, *Angew. Chem., Int. Ed.*, 2024, **63**, e202406796.
15 Y. Wang, N. Alaslai, B. Ghanem, X. Ma, X. Hu, M. Balcik, Q. Liu, M. A. Abdulhamid, Y. Han, M. Eddaoudi and I. Pinnau, *Adv. Mater.*, 2024, **36**, 2406076.
16 Y. Zhao, E. M. Rettner, K. L. Harry, Z. Hu, J. Miscall, N. A. Rorrer and G. M. Miyake, *Science*, 2023, **382**, 310–314.
17 L. P. Manker, M. A. Hedou, C. Broggi, M. J. Jones, K. Kortsen, K. Puvanenthiran, Y. Kupper, H. Frauenrath, F. Marechal, V. Michaud, R. Marti, M. P. Shaver and J. S. Luterbacher, *Nat. Sustain.*, 2024, **7**, 640–651.
18 N. Blagojevic, S. Das, J. Xie, O. Dreyer, M. Radjabian, M. Held, V. Abetz and M. Müller, *Adv. Mater.*, 2024, **36**, 2404560.
19 T. Eck and H. F. Gruber, *Macromol. Chem. Phys.*, 1994, **195**, 3541–3565.
20 C. Hamciuc, E. Hamciuc, D. Serbezeanu, T. Vlad-Bubulac and M. Cazacu, *Polym. Int.*, 2011, **60**, 312–321.
21 R. Sawada and S. Ando, *Macromolecules*, 2022, **55**, 6787–6800.
22 P. Suvannasara, S. Tateyama, A. Miyasato, K. Matsumura, T. Shimoda, T. Ito, Y. Yamagata, T. Fujita, N. Takaya and T. Kaneko, *Macromolecules*, 2014, **47**, 1586–1593.

23 C.-K. Chen, Y.-C. Lin, L.-C. Hsu, J.-C. Ho, M. Ueda and W.-C. Chen, *ACS Sustainable Chem. Eng.*, 2021, **9**, 3278–3288.
24 C. Zhang, X. He and Q. Lu, *Eur. Polym. J.*, 2023, **200**, 112544.
25 Y.-K. Su, G. N. Short and S. A. Miller, *Green Chem.*, 2023, **25**, 6200–6206.
26 W. He, J. Lan, X. Huang and J. Shang, *J. Appl. Polym. Sci.*, 2014, **131**, 40807.
27 B. Liu, C. Liu, H. G. De Luca, S. K. Raman Pillai, D. B. Anthony, J. Li, A. Bismarck, M. S. P. Shaffer and M. B. Chan-Park, *Polym. Chem.*, 2019, **10**, 1324–1334.
28 Z. Wu, Y. Peng, Y. Song, H. Liang, L. Gong, Z. Liu, Q. Zhang and Y. Chen, *Mater. Today Energy*, 2023, **32**, 101243.
29 G. Chen, D. Li, L. Chen, Z. Lin, W. Li, B. Zhao, Z. Zhao, J. Liu, Y. Sun, J. Pang and Z. Jiang, *Chem. Eng. J.*, 2024, **500**, 156642.
30 Y. Yu, W. Zhu, H. Li, J. Long, W. Huang, J. Li, L. Chen and Y. Zhang, *Eur. Polym. J.*, 2024, **203**, 112653.
31 K. R. Carter, R. A. DiPietro, M. I. Sanchez, T. P. Russell, P. Lakshmanan and J. E. McGrath, *Chem. Mater.*, 1997, **9**, 105–118.
32 W. Volksen, J. L. Hedrick, T. P. Russell and S. Swanson, *J. Appl. Polym. Sci.*, 1997, **66**, 199–208.
33 M. Kuang, H. Duan, J. Wang and M. Jiang, *J. Phys. Chem. B*, 2004, **108**, 16023–16029.
34 M. Kluge, H. Rennhofer, H. C. Lichtenegger, F. W. Liebner and T. Robert, *Eur. Polym. J.*, 2020, **129**, 109622.
35 F. Van Lijsebetten, Y. Spiesschaert, J. M. Winne and F. E. Du Prez, *J. Am. Chem. Soc.*, 2021, **143**, 15834–15844.
36 Q. Cai, T. Bai, H. Zhang, X. Yao, J. Ling and W. Zhu, *Mater. Today*, 2021, **51**, 155–164.
37 Q. Cai, X. Li and W. Zhu, *Macromolecules*, 2020, **53**, 2177–2186.
38 Q. Luan, H. Hu, X. Jiang, C. Lin, X. Zhang, Q. Wang, Y. Dong, J. Wang and J. Zhu, *J. Hazard. Mater.*, 2023, **457**, 131801.
39 H. Zhang, M. Jiang, Y. Wu, L. Li, Z. Wang, R. Wang and G. Zhou, *Green Chem.*, 2021, **23**, 2437–2448.
40 O. Platnieks, S. Gaidukovs, V. Kumar Thakur, A. Barkane and S. Beluns, *Eur. Polym. J.*, 2021, **161**, 110855.
41 H. Kim, H. Jeon, G. Shin, M. Lee, J. Jegal, S. Y. Hwang, D. X. Oh, J. M. Koo, Y. Eom and J. Park, *Green Chem.*, 2021, **23**, 2293–2299.
42 H. Kwak, H. Kim, S.-A. Park, M. Lee, M. Jang, S. B. Park, S. Y. Hwang, H. J. Kim, H. Jeon, J. M. Koo, J. Park and D. X. Oh, *Adv. Sci.*, 2023, **10**, 2205554.
43 J. Yang, P. Pan, L. Hua, Y. Xie, T. Dong, B. Zhu, Y. Inoue and X. Feng, *Polymer*, 2011, **52**, 3460–3468.
44 K. Wang, T. Jiao, Y. Wang, M. Li, Q. Li and C. Shen, *Mater. Lett.*, 2013, **92**, 334–337.
45 O. Platnieks, S. Gaidukovs, N. Neibolts, A. Barkane, G. Gaidukova and V. K. Thakur, *Mater. Today Chem.*, 2020, **18**, 100351.